FAST v8 Verification and Validation Using Experiments from Aeroelastically Tailored Megawatt-Scale Wind Turbine Blades

Preprint

Sirnivas Guntur, Jason Jonkman, Scott Schreck, Bonnie Jonkman, Qi Wang, and Michael Sprague
National Renewable Energy Laboratory

Michael Hind and Ryan Sievers
Siemens Energy Inc.

Presented at the American Institute of Aeronautics and Astronautics Science and Technology Forum and Exposition (SciTech 2016)
San Diego, California
January 4–8, 2016

NREL is a national laboratory of the U.S. Department of Energy
Office of Energy Efficiency & Renewable Energy
Operated by the Alliance for Sustainable Energy, LLC

This report is available at no cost from the National Renewable Energy Laboratory (NREL) at www.nrel.gov/publications.

Conference Paper
NREL/CP-5000-65389
January 2016

Contract No. DE-AC36-08GO28308

NOTICE

This report is available at no cost from the National Renewable Energy Laboratory (NREL) at www.nrel.gov/publications.

Available electronically at SciTech Connect http:/www.osti.gov/scitech

Available for a processing fee to U.S. Department of Energy and its contractors, in paper, from:

U.S. Department of Energy
Office of Scientific and Technical Information
P.O. Box 62
Oak Ridge, TN 37831-0062
OSTI http://www.osti.gov
Phone: 865.576.8401
Fax: 865.576.5728
Email: reports@osti.gov

Available for sale to the public, in paper, from:

U.S. Department of Commerce
National Technical Information Service
5301 Shawnee Road
Alexandria, VA 22312
NTIS http://www.ntis.gov
Phone: 800.553.6847 or 703.605.6000
Fax: 703.605.6900
Email: orders@ntis.gov

Cover Photos by Dennis Schroeder: (left to right) NREL 26173, NREL 18302, NREL 19758, NREL 29642, NREL 19795.

NREL prints on paper that contains recycled content.

FAST v8 Verification and Validation for a Megawatt-Scale Wind Turbine with Aeroelastically Tailored Blades*

Srinivas Guntur[†], Jason Jonkman[‡], Scott Schreck[§], Bonnie Jonkman[¶], Qi Wang[k], and Michael Sprague[¶]
National Renewable Energy Laboratory, Golden, CO

Michael Hind[**] and Ryan Sievers[††]
Siemens Energy Inc., Boulder, CO.

This paper presents findings from a verification and validation exercise on the latest version of the Department of Energy/National Renewable Energy Laboratory wind turbine aeroelastic engineering simulation tool FAST. Results from a set of 1141 FAST simulations were compared to those from the Siemens' aeroelastic simulation tool BHawC, as well as experimental data from a heavily instrumented 2.3 megawatt Siemens wind tur- bine located at the National Wind Technology Center. The code validation was performed following the IEC-61400-13 standard, where a set of select quantities of interest from simulations at various wind speeds and atmospheric turbulence conditions were used for a three-way comparison between FAST, BHawC, and the measurements. Results highlight many improvements of the latest version of FAST over its previous versions. This paper also provides comments from the authors on the data quality, and avenues for potential future work using these results.

I. Introduction

This paper presents a verification and validation of the latest version of the U.S. Department of Energy's open-source wind turbine aero-elastic simulation tool FAST (version 8), developed and supported by the National Renewable Energy Laboratory (NREL). Recent efforts in FAST development have involved many new modifications to the tool, including a new modularization framework[1, 2] and new capabilities for modeling advanced blades with aero-elastic tailoring.[3, 4] Verification and validation is centered on the Siemens 2.3 megawatt (MW) turbine with a 108-m rotor that is stationed at NREL's National Wind Technology Center (NWTC). The turbine is heavily instrumented, and measurement data have been made available through a collaborative research activity between NREL and Siemens Energy. Data were collected over a period of several months under normal operating conditions for a range of wind speeds and turbulence intensities, and these data were used in this validation exercise. Validation was conducted following the guidelines stipulated in the International Electrotechnical Commission (IEC) wind turbine loads-measurement standard 61400-13.[5] Code-to-code verification was accomplished with a comparison of FAST v8 simulation results with those of the Siemens aeroelastic simulation tool, BHawC.

[†]Post-Doc, National Wind Technology Center, 15013 Denver West Pkwy, Golden, CO 80401, AIAA Member.
[‡]Senior Engineer, National Wind Technology Center, 15013 Denver West Pkwy, Golden, CO 80401, AIAA Member.
[§]Principle Engineer, National Wind Technology Center, 15013 Denver West Pkwy, Golden, CO 80401, AIAA Member.
[¶]Senior Scientist, National Wind Technology Center, 15013 Denver West Pkwy, Golden, CO 80401, AIAA Member.
[k]Engineer, National Wind Technology Center, 15013 Denver West Pkwy, Golden, CO 80401, AIAA Member.
[**]Engineer, Siemens Energy Inc., Boulder, CO 80302.
[††]Principle Engineer, Siemens Energy Inc., Boulder, CO 80302.

FAST is an open-source multi-physics simulation tool for the design and analysis of advanced land- based and off-shore wind technology. Underpinning FAST is a modularization framework that enables coupling of various modules, each representing different physics domains of the wind system.[1, 2] FAST v8 includes a mesh-mapping utility allowing each module to be independently discretized in space and time, and a mathematically rigorous solution procedure supporting loose coupling of modules with implicit- coupling relations. For land-based turbine simulations, FAST has modules for wind inflow (InflowWind); aerodynamics (AeroDyn); control and electrical-drive dynamics (ServoDyn); and blade, drivetrain, nacelle, tower, and platform structural dynamics (ElastoDyn).

In the newest release of FAST, BeamDyn, a new blade-dynamics module has been introduced and the AeroDyn aerodynamics module has been overhauled to support the analysis of advanced aero-elastically tailored blades.[3, 4] BeamDyn is based on geometrically exact beam theory (GEBT) and is implemented using Legendre spectral finite elements. The model includes full geometric nonlinearity supporting large deflection, with bending, torsion, shear, and extensional degrees of freedom (DOF); anisotropic composite material couplings (using full 6x6 mass and stiffness matrices, including bend-twist coupling); and a reference axis that permits blades that are not straight (supporting built-in curve, sweep, and sectional offsets). When these advanced features are needed, BeamDyn replaces the more simplified blade structural model of ElastoDyn, which is only applicable to straight isotropic blades dominated by bending.

Also in the new FAST v8, AeroDyn has been overhauled to (1) fix underlying problems with the original theoretical treatments, (2) introduce improved skewed-wake and unsteady airfoil aerodynamics models[a] , (3) enable modeling of highly flexible and non-straight blades, and (4) support the unique features of the FAST modularization framework.[4, 6]

II. Methods

The NWTC is home to several MW-scale test turbines. One of these is a Siemens 2.3-MW machine[7] (SWT-2.3-108) that operates in an upwind configuration and is equipped with a 3-bladed, 108-m-diameter rotor. It is a variable-speed turbine operating under a collective pitch control, and the rotor is connected to the generator via a gearbox. The blades used on this machine have a prebent geometry, i.e., the blade shape under no-load conditions is not straight, but curved. Additionally, these blades are flexible, aeroelastically tailored and incorporate bend-twist-coupling. This turbine is instrumented with FiberBragg strain sensors capable of measuring blade tip deflections; surface pressure taps; strain gauges at the blade root, tower top, and the tower base; and a data acquisition system that records turbine operating data like the rotor speed and the electrical power output. Wind speed and direction are measured by sensors mounted on an upwind meteorological tower. Measurements on this heavily instrumented turbine have been collected and shared as a part of a cooperative research project between NREL and Siemens Energy. This unique set of measurements is well suited for validation of high-fidelity blade structural modeling tools, like BeamDyn within FAST v8, and will facilitate a wide variety of research possibilities. In the current work, the comparisons between FAST and BHawC predictions and the measurements will be discussed for various turbine operating conditions consistent with the recommendations in the IEC 61400-13 standard.

Several months of test data were recorded on the Siemens 2.3-MW wind turbine and the NWTC 135-m meteorological tower. The meteorological tower is located approximately 2.5 rotor diameters upstream of the turbine and is instrumented with several sensors along its length that measure the wind speed, wind direction, and atmospheric pressure. The inflow wind speed data used in this analysis were recorded at 80 m, which is close to the turbine hub height. Each 10-min data set contains surface pressure measurement data, strain gage data, turbine operation data, and the inflow data from the met tower. In total, several months of data have been recorded, of which this report presents data from 1141 10-min datasets (i.e., approximately 48 hours of data). The data samples were selected based on their mean hub-height wind speed and turbulence intensities in order to populate the recommended test matrix of the IEC 61400-13; see Table 1. While the 1141 simulations were run according to Table 1, the results plotted in Section III are binned only by wind speed. Overall, these data represent operating conditions with inflow velocities between the turbine's cut-in and the cut-out wind speeds, at various inflow turbulence intensity levels, up to approximately 23%.

[a] Unsteady aerodynamics have not been included in the present simulations, and it is anticipated that this submodule will be functional in the future release of FAST.

Each bin in the shown test matrix contains several 10-min datasets. For each dataset, the minimum, maximum, mean, and standard deviation of the following quantities of interest (QoI) are determined from both the simulations and the measured data:

- Rotor speed
- Electrical power
- Blade-root bending moments (in and out of the rotor plane)
- Main-shaft bending moments (yaw and tilt directions, in a non-rotating coordinate system)
- Tower-top torsional moment
- Tower-bottom bending moments (parallel and perpendicular to the wind direction)
- Blade-tip deflections (in and out of the rotor plane)

	Mean Wind Speed [m/s]														
Turbulence	Region 2								v (rated)	Region 3					
Intensity (%)	3.5-4.5	4.5-5.5	5.5-6.5	6.5-7.5	7.5-8.5	8.5-9.5	9.5-10.5	10.5-11.5	11.5-12.5	12.5-14	14-16	16-18	18-20	20-22	22-24
< 3	0	4	6	3	0	0	0	0	0	0	0	0	0	0	0
3-5	0	20	19	19	9	5	1	1	0	0	0	0	0	0	0
5-7	0	32	50	32	14	3	7	3	2	2	0	0	0	0	0
7-9	0	43	39	44	17	17	3	7	2	2	2	0	1	0	1
9-11	0	32	42	35	29	13	7	11	9	5	9	5	0	0	1
11-13	0	22	21	16	16	9	12	15	16	14	15	6	4	1	0
13-15	0	2	16	25	10	6	14	15	24	11	15	14	5	1	0
15-17	0	1	10	11	6	4	7	12	12	10	18	8	9	2	0
17-19	0	2	12	6	0	2	3	12	4	10	8	7	5	0	0
19-21	0	2	3	3	2	1	3	1	4	2	3	1	0	0	0
21-23	0	0	0	1	0	0	0	0	0	1	0	0	0	0	0
Sum	0	160	218	195	103	60	57	77	73	57	70	41	24	4	2

Table 1: IEC matrix populated with the measured data. Numbers represent the number of 10-minute data sets within each bin, for a total of 1141.

FAST model of the SWT-2.3-108 machine

The FAST model of the SWT-2.3-108 machine was created based on the information obtained from Siemens, as well as the inflow data from the experimental database, for each of the cases simulated. This three-bladed upwind turbine has a fixed coning angle of 5° and a rotor tilt angle of 6° , both directing the blades away from the tower. The tower, blades and the main shaft are modeled as elastic bodies with properties obtained from Siemens, and the tower base was fixed.

In the new BeamDyn, it is possible to model a blade defined by many cross-sectional property stations with relatively few node points for integration while capturing all of the provided material properties; see Wang et al.[8] The cross-sectional properties of the blades on the Siemens machine were defined at 106 stations along its length. For BeamDyn spectral finite element calculations (e.g., those for mass and stiffness matrices), these data were spatially integrated using the trapezoidal rule and each blade was discretized using a single seventh-order spectral finite element. In contrast to the nonlinear finite-element implementation of BeamDyn in FAST, the structural model of BHawC employs a co-rotational beam formulation, which is a combined mutli body and linear finite-element representation allowing for geometric nonlinearities through a series of multiple bodies, each composed of linear finite elements. In the BHawC model of the SWT-2.3-108 machine used in this study, the blade was discretized into 16 linear elements.

The 2D airfoil aerodynamic properties of the airfoil geometries in the blade were obtained from Siemens. The blade was modeled in AeroDyn using 20 nodes. The lift-coefficient data were processed to include rotational augmentation effects in the same way as BHawC, according to a variation of the Snel[9] model.

The measured yaw error in most test cases was very small, with a few exceptions of yaw errors higher than 5° (based on a 10-minute average of the wind direction sensor readings obtained from the upwind met tower). Both BHawC and FAST simulations take this into account. In the FAST simulations, a fixed nacelle yaw error with a value equal to the 10-min average yaw error for each case was used.

The new InflowWind supports several wind file formats. In the simulations presented herein, FAST used the same turbulent inflow input files as BHawC, which used HawC-style turbulence boxes. For each case simulated, the turbulence box is scaled according to the mean wind speed and the turbulence intensity at the turbine hub height, obtained from the 80-m wind speed and direction measurement from the met tower. In the FAST simulations, shear was modeled using the power-law exponent of 0.2, following the IEC 61400-13 guidelines. BHawC simulations used atmospheric shear estimates based on LIDAR measurements, and so there may be differences between the inflow

conditions of the test turbine, FAST simulations, and the BHawC simulations, adding to the uncertainty in this exercise.

A controller in a Bladed-style DLL form obtained from Siemens was used for pitch and torque control in the FAST simulations. It is known that this DLL controller does not employ the exact same control logic as the physical turbine or the BHawC simulations, but is similar. Some inaccuracy in the FAST results from the use of this controller is possible. It must also be noted here that the drivetrain damping used in the FAST simulations presented in this paper are higher than those in the Siemens turbine specification. This was manually altered to overcome a drive train resonance that was being detected in the initial FAST simulations. This is an issue that is currently being investigated, and will be addressed in future.

The simulations shown in this work were generated using FAST v8.12.01a-bjj compiled in double precision with:

- ElastoDyn v1.03.00a-bjj
- BeamDyn v1.00.01
- AeroDyn v15.00.00a-bjj
- InflowWind v3.01.00a-adp
- ServoDyn v1.03.01a-bjj

Each 10-min test case was simulated using three different FAST configurations, to be able to analyze the relative improvements in FAST between the capabilities in its previous public releases (FAST v8.10 and earlier) and the current developments with BeamDyn and AeroDyn. The three sets of simulations presented in this paper are:

1. FAST with straight ElastoDyn blades and straight AeroDyn blades,
2. FAST with straight ElastoDyn blades and curved AeroDyn blades, and
3. FAST with curved BeamDyn blades and curved AeroDyn blades.

The FAST simulations with BeamDyn used an integration time increment of 0.0005s, while those with ElastoDyn used 0.005s. All FAST simulations were carried out for 12 minutes, and the first two minutes of the results were ignored to take out any effects of initial transients. BHawC simulations were 11 minutes long with a 0.02s integration time increment, and the first minute of transience was ignored in processing the BHawC results.

Note that the structural blade in ElastoDyn is straight and only includes bending DOFs, whereas the structural blade in BeamDyn is curved and includes the DOFs bending, torsion, shear, and extension, with composite coupling terms. This way, the relative improvements between the previous vs. newer capabilities of AeroDyn, and the improvements between ElastoDyn vs. BeamDyn for blades are investigated.

III. Results

The plots presented herein show the mean and standard deviation of the individual 10-min samples as well as the binned average means of the 1141 cases simulated. The y-axes in the Figures 5 to 2 have been removed to protect Siemens proprietary data, and so this paper will present a discussion based only on the noticeable relative trends between the different data shown. Each figure shows four different comparisons of the same QoI. Subfigures (a) and (b) show a comparison of the data from FAST with BeamDyn, BHawC and experimental results, while the subfigures (c) and (d) show those comparing FAST with BeamDyn with FAST with ElastoDyn. Subfigures (a) and (c) show the means of the individual 10-min data, while the subfigures (b) and (d) show the binned average means of the same QoIs, and the standard deviations calculated from the individual 10-min data in a given bin. The data points connected by a line indicate the mean value of the binned data, calculated as the average of the means of the individual 10-min simulations within that bin. The scatter above and below each of the mean data shows one standard deviation of the individual 10-min data sets in that bin added and subtracted to the mean of that bin.
The explanations for the different curves shown in the legend of these plots are as follows:

- Data - experimental measurements
- BHawC - results from Siemens' BHawC simulations
- FAST (straight AD) - FAST simulations with ElastoDyn and a straight aerodynamic blade
- FAST (curved AD) - FAST simulations with ElastoDyn and a curved aerodynamic blade (this is a new capability introduced in AeroDyn v15).
- FAST (BD) - FAST simulations with the new BeamDyn and a curved aerodynamic blade.

Note that 'ElastoDyn' and 'BeamDyn' designate structural modules used to model the blades only; the structural dynamics of the remainder of the turbine (drivetrain, nacelle and tower) were always modeled in ElastoDyn.

Discussion of the results

Overall, the results indicate that the predictions from the latest version of FAST compare consistently well with those of BHawC as well as the experimental data. A comparison between the results from various FAST simulations indicates that FAST simulations with BeamDyn improve significantly over FAST simulations with ElastoDyn. A comparison between FAST simulations with ElastoDyn with curved versus straight aerodynamic blades reveals no significant differences between the two.

Figure 1 and 2 show the electrical power and the rotor speed, respectively. As mentioned earlier, note that each point in the scatter shown in subfigures (b) and (d) in this paper represents the standard deviation of the time series of an individual 10-min data set, added and subtracted to the mean of that bin. The agreement between the different data in electrical power is excellent. The rotor speed is also very close but does show a small deviation between FAST and BHawC. This small difference could be due to a slightly different total aerodyanmic torque generated by the flexible blades in BHawC and FAST, or due to a minor difference in the controllers used by FAST, BHawC, and the physical turbine. From Figures 1a and 2a, it can also be seen that there are some isolated cases in region 2 where the rotor speed and electrical power deviate from the general trend for this turbine, and it is worthwhile to note that these data have some influence on the variance in the loads data presented next. Even so, the agreement in electrical power and the rotor speed between FAST, BHawC, and the experimental data is close enough to assure that a majority of the turbine operating conditions being simulated and compared across FAST, BHawC, and the measurements are similar.

Figures 3 and 4 show the in-plane and the out-of-plane blade-tip deflections from the simulations and the experimental measurements. The blade-tip deflection was not measured directly, but rather it was estimated using the FiberBragg strain measurements from several locations along the span of Blade B. The local curvature was estimated from the strain measurements, which were then used to calculate the instantaneous shape of the blade. By integrating the shape, the magnitudes of the blade tip deflections, in and out of the rotor plane, were obtained. As explained earlier, one of the main reasons for the high fidelity beam model BeamDyn is to facilitate accurate modeling of large flexible rotor blades. From Figures 3c and 4c, a significant difference between BeamDyn and ElastoDyn is visible. This difference is in fact an improvement, as revealed by Figures 3a and 4a. The agreement of FAST with BeamDyn with the measurements as well as BHawC is very good thoughout regions 2 and 3, and the agreement with the experimental data is particularly good in region 3. These figures show that BeamDyn is a significant improvement over ElastoDyn.

Figures 5 and 6 show the in-plane and out-of-plane blade-root bending moments, respectively. Experimental data for the blade-root bending moments consist of strain-gage measurements at the roots of all three blades. For simplicity, only data from one of the three blades (Blade A) are being shown for the blade-root bending moments in this study. From the comparisons shown in Figures 5a and 5b, fairly good agreement can be seen between the BHawC, experimental, and the FAST (with BeamDyn) data. The in-plane blade-root bending moment is heavily sinusoidal, i.e., the amplitude of the oscillations is much higher than the mean, which is the reason why the standard deviations shown in Figure 5b are so far away from the mean. From the out-of-plane blade-root bending moments shown in Figures 6b and 6d, the overall agreement between FAST (with BeamDyn), BHawC, and the measurements appears to be good. A small difference between the FAST results and the Siemens data is discernible, which may most likely be related to the small difference in the rotor speed also seen between FAST and Siemens data in Figure 2 as discussed earlier. Furthermore, from Figures 6c and 6d the improvement of FAST simulations with BeamDyn over ElastoDyn is clearly visible, more so at higher wind speeds.

Figures 7 and 8 show the main shaft bending moments along the turbine yaw and tilt directions, respectively. The experimental data for these QoIs were acquired using a strain sensor mounted on the rotating shaft, which are then converted to a non-rotating coordinate system by a transformation using the azimuthal position of the rotor. Due to the geometry of the hub-to-shaft interface for this particular turbine, this measurement is challenging to make and so measurement uncertainty is increased for this comparison. Furthermore, the shaft moments are also influenced by the vertical wind shear, which has some inherent epistemic uncertainty associated with it (i.e., the uncertainty that arises due to lack of knowledge of the source of the variability in the data[10]), as mentioned in the previous section. This uncertainty, when coupled with the standard deviation in the measurements shown in Figures 7b and 8b, makes it challenging to com- pare the mean values of the measurements and the model data. Regardless, the mean values of this QoI also indicate a better match between FAST with BeamDyn and the data, as opposed to FAST with ElastoDyn.

Figures 9 and 10 show the tower-bottom bending moments in the side-side and fore-aft directions, respectively. As is visible from Figures 10a and 10c, while ElastoDyn results show a higher tower fore-aft moment compared to BeamDyn results, BeamDyn results match quite well with BHawC and the experimental data. This is another indication that FAST with BeamDyn shows improvement over FAST with ElastoDyn. Figures 9b and 9d reveal high standard deviations on this quantity from FAST simulations with BeamDyn. It has been observed that FAST with BeamDyn results show a tower side-to-side and drivetrain coupled mode not found in other FAST or BHawC models, that is believed to be causing this increased variance in this QoI. The reason why this exists in FAST with BeamDyn and not in FAST with ElastoDyn, BHawC, or experiments is currently unknown, but will be looked into in future work.

Figure 11 shows the tower-top torsional moment. At lower wind speeds, the agreement between FAST with BeamDyn and the experimental data is very good. At rated and above rated wind speeds there seems to be a good agreement between the FAST with BeamDyn and the BHawC results, but it also shows a deviation from the data. In this case, too, the standard deviations of the data are much larger than the means. It is noteworthy to mention here that some uncertainty in the sensor calibration for this particular channel had been identified previously. Once again, these measurements are sensitive to the vertical shear as well as the yaw error of the turbine, along with the difficulty associated with experimental measurement of this QoI, making a comparison of the means challenging.

IV. Conclusion

In this paper, the latest results from FAST v8 with the new BeamDyn and AeroDyn modules have been presented. The release of BeamDyn and the AeroDyn overhaul within FAST v8 opens up new possibilities in modeling and designing advanced aero-elastically tailored blades. Following the IEC-61400-13 standard as a guideline, a comparison has been presented between FAST with and without its latest improvements, Siemens' in-house code BHawC, and the experimental data that were acquired from a series of field-test measurements from the Siemens 2.3-MW wind turbine at NWTC. The analysis included only low yaw errors and modest wind speed variations, associated with normal turbine operation conditions. Results revealed significant improvements in the modeling capabilities of the latest version of FAST over its previous capabilities.

The results also revealed some uncertainties that are inherent to the experimental data acquisition process as well as the modeling and simulation process, analysis of which will be a part of future work. In addition, validation in conditions with elevated yaw errors and wind speed variations, both associated with extreme conditions, correspond to disparate physics and numerics and require special considerations, which will also be a part of future work.

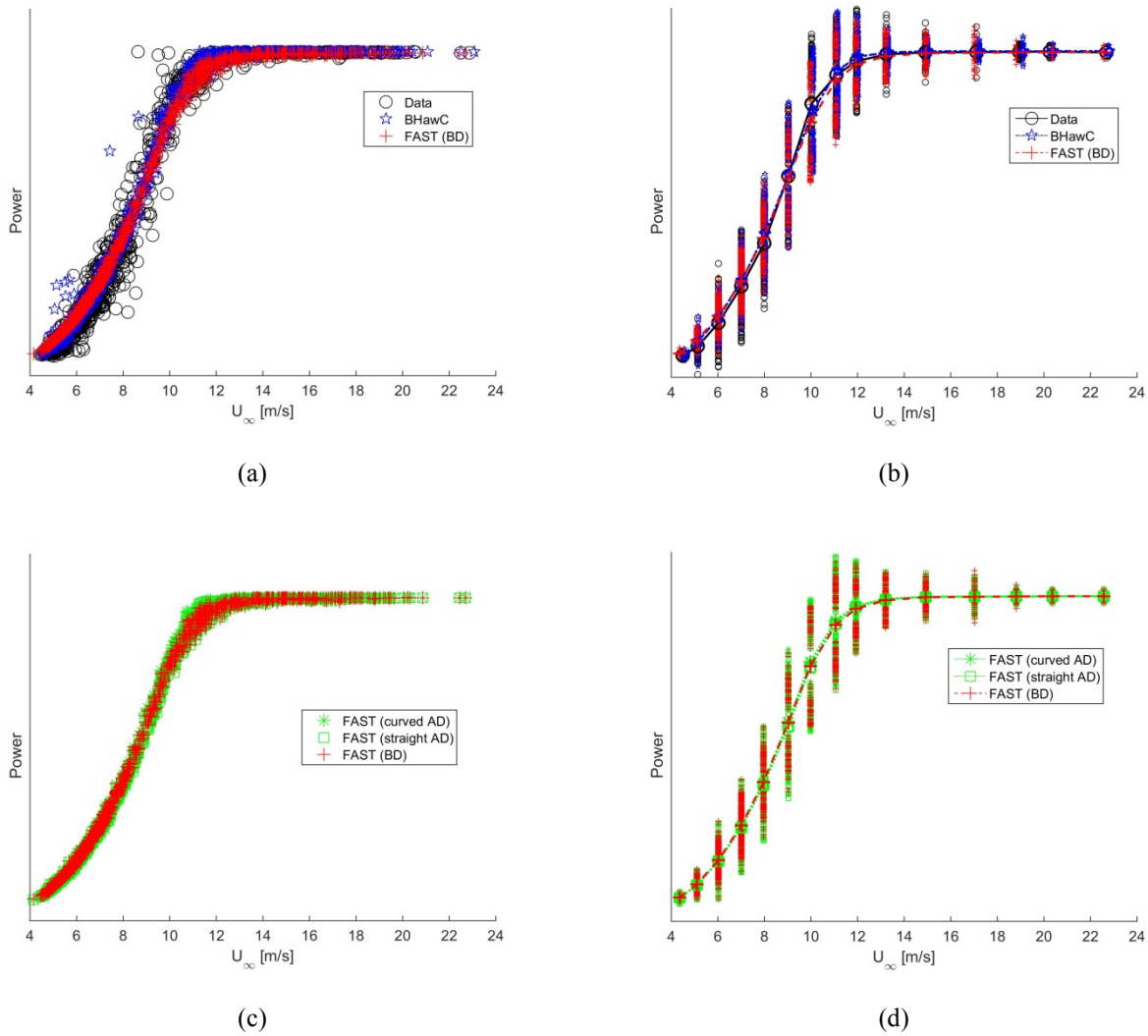

Figure 1: Electrical power.
(a) Individual 10-min averages from experimental data, BHawC, and FAST (BD).
(b) Binned averages of data in (a) are denoted by points connected by lines; the scatter above and below these data denote plus or minus one standard deviation, respectively, of the individual 10-min data sets in that bin.
(c) Individual 10-min averages from FAST (BD), FAST (straight AD), and FAST (curved AD).
(d) Binned averages of data in (c) are denoted by the points connected by lines; the scatter above and below these data denote plus or minus one standard deviation, respectively, of the individual 10-min data sets in that bin.

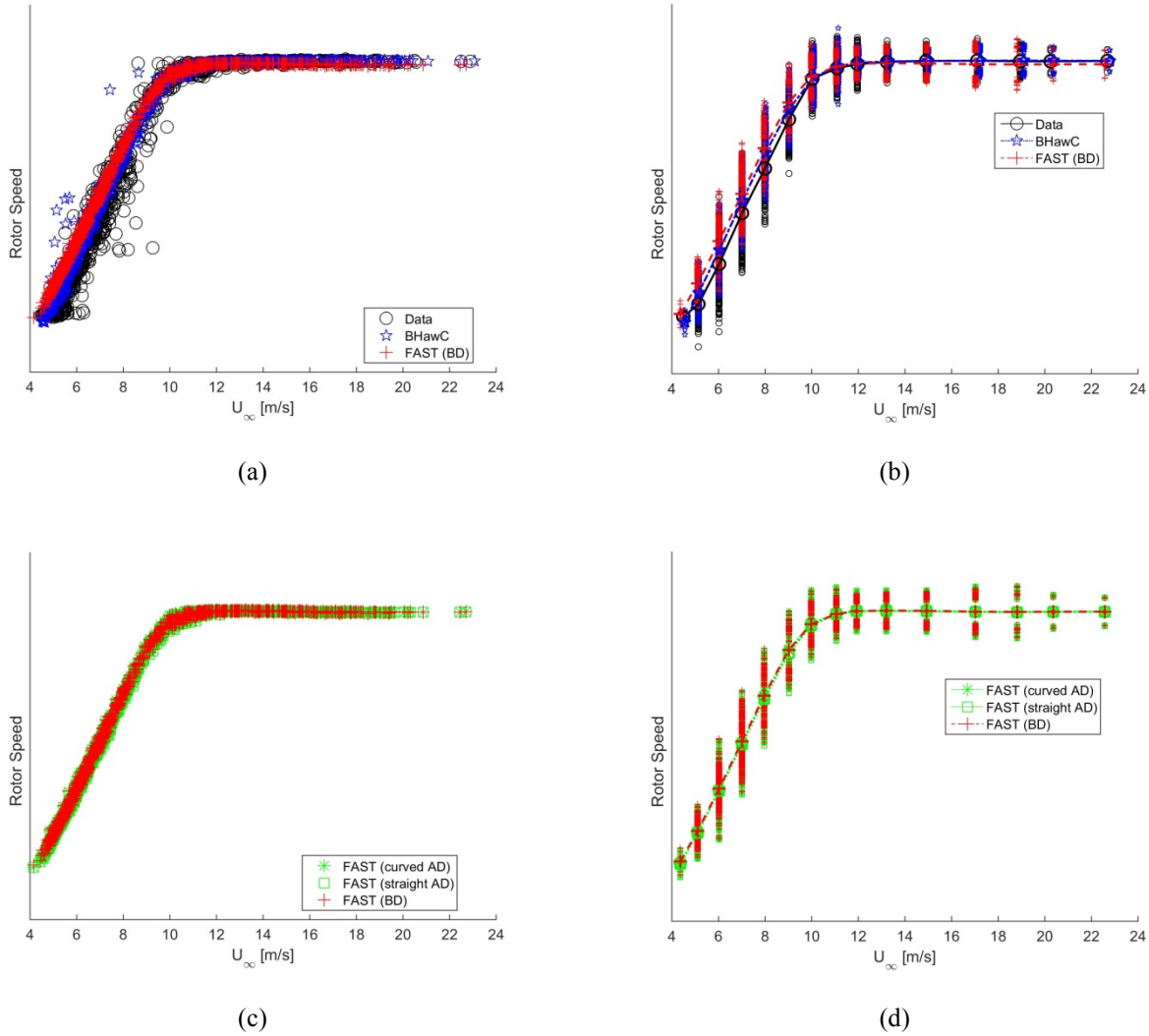

Figure 2: Rotor speed.
(a) Individual 10-min averages from experimental data, BHawC, and FAST (BD).
(b) Binned averages of data in (a) are denoted by points connected by lines; the scatter above and below these data denote plus or minus one standard deviation, respectively, of the individual 10-min data sets in that bin.
(c) Individual 10-min averages from FAST (BD), FAST (straight AD), and FAST (curved AD).
(d) Binned averages of data in (c) are denoted by the points connected by lines; the scatter above and below these data denote plus or minus one standard deviation, respectively, of the individual 10-min data sets in that bin.

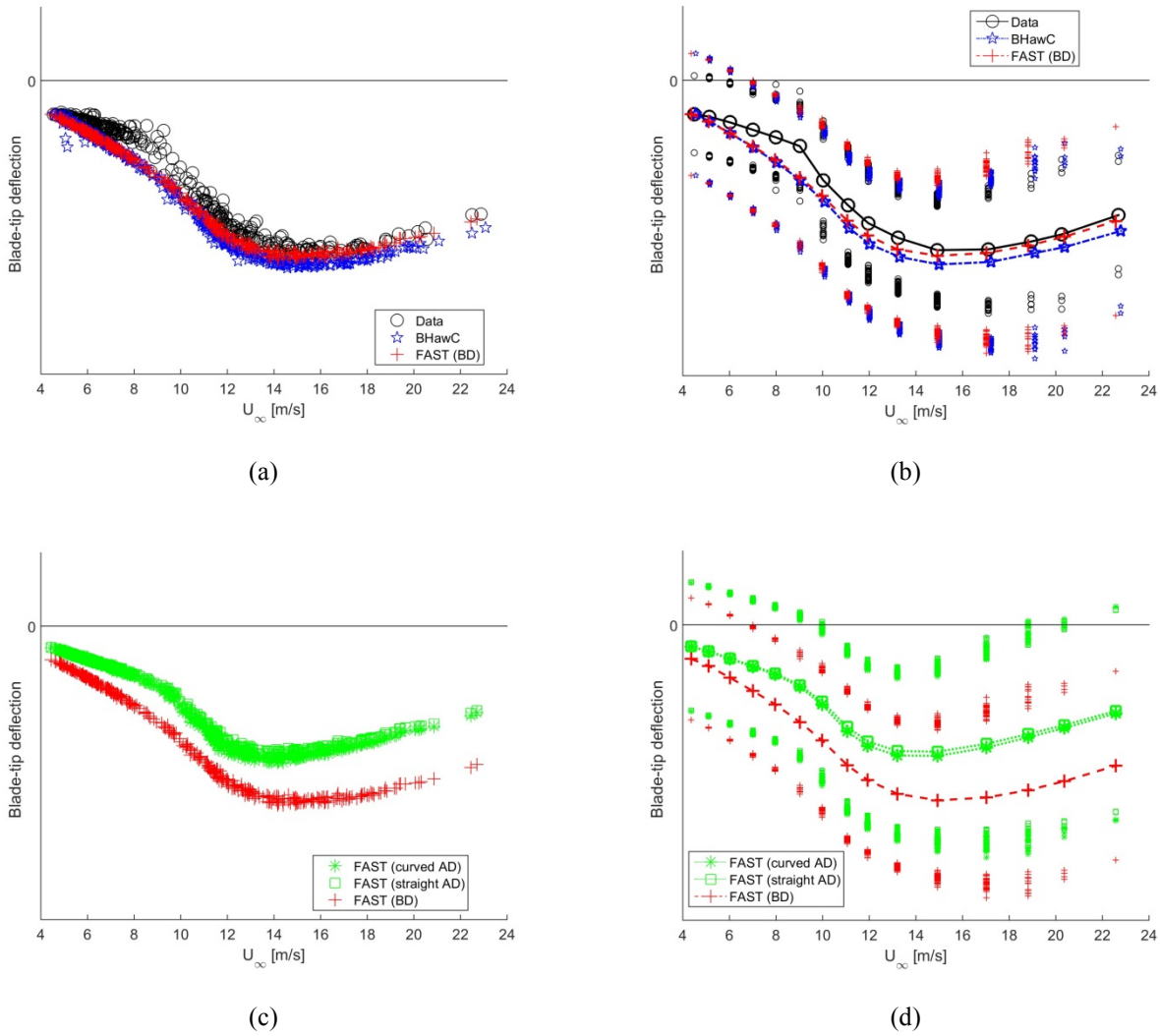

Figure 3: Blade in-plane tip deflections.
(a) Individual 10-min averages from experimental data, BHawC, and FAST (BD).
(b) Binned averages of data in (a) are denoted by points connected by lines; the scatter above and below these data denote plus or minus one standard deviation, respectively, of the individual 10-min data sets in that bin.
(c) Individual 10-min averages from FAST (BD), FAST (straight AD), and FAST (curved AD).
(d) Binned averages of data in (c) are denoted by the points connected by lines; the scatter above and below these data denote plus or minus one standard deviation, respectively, of the individual 10-min data sets in that bin.

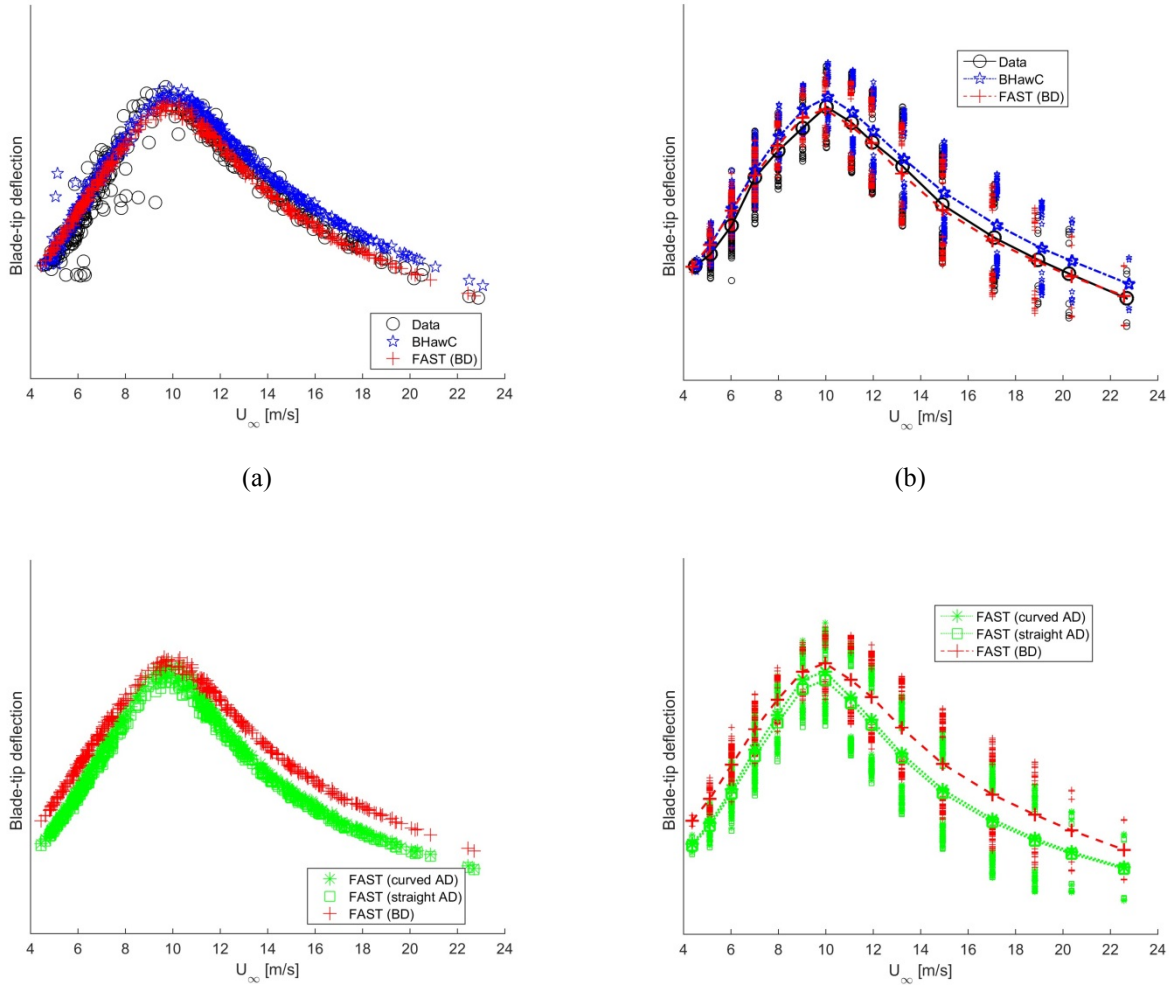

Figure 4: Blade out-of-plane tip deflections.
(a) Individual 10-min averages from experimental data, BHawC, and FAST (BD).
(b) Binned averages of data in (a) are denoted by points connected by lines; the scatter above and below these data denote plus or minus one standard deviation, respectively, of the individual 10-min data sets in that bin.
(c) Individual 10-min averages from FAST (BD), FAST (straight AD), and FAST (curved AD).
(d) Binned averages of data in (c) are denoted by the points connected by lines; the scatter above and below these data denote plus or minus one standard deviation, respectively, of the individual 10-min data sets in that bin.

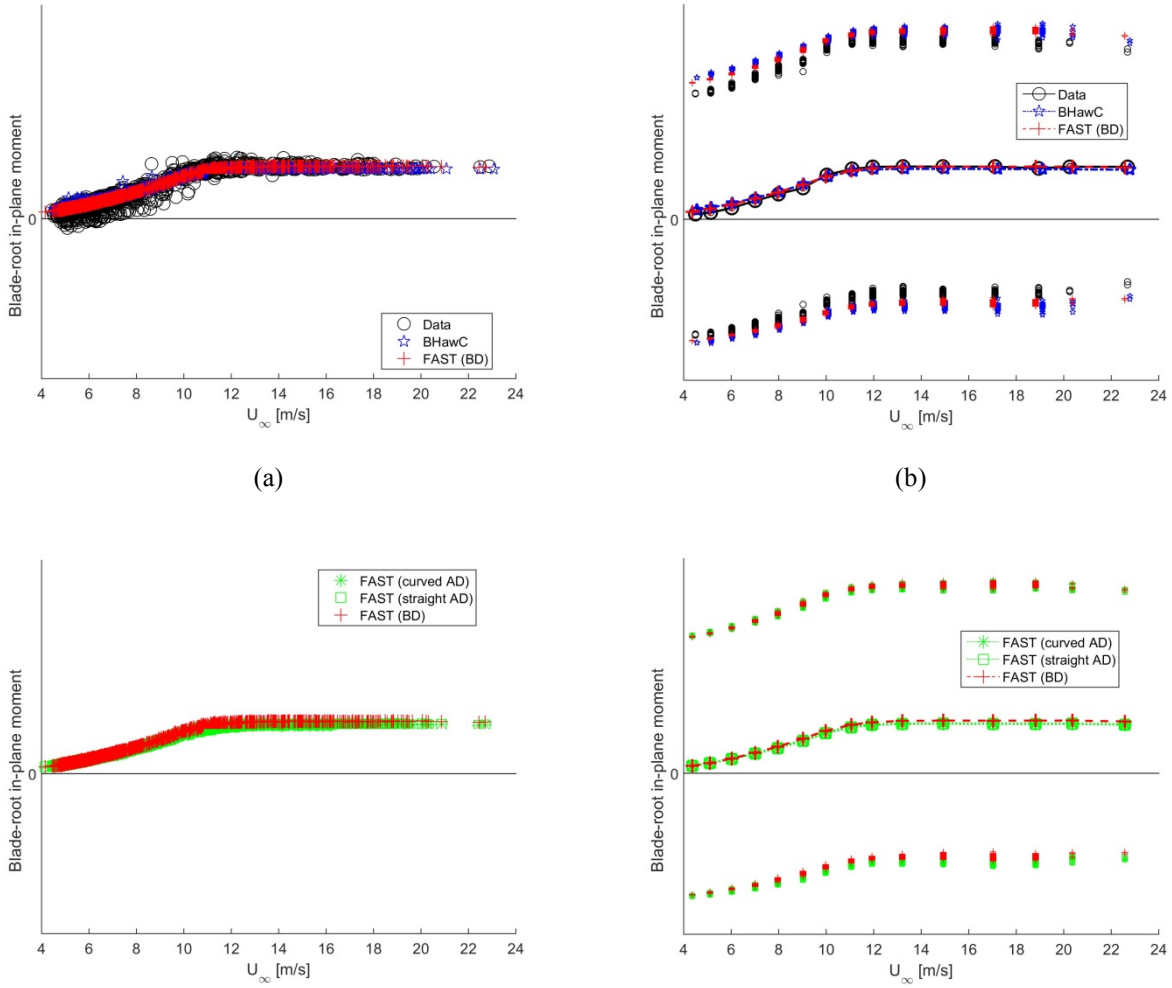

Figure 5: Blade-root in-plane bending moments.
(a) Individual 10-min averages from experimental data, BHawC, and FAST (BD).
(b) Binned averages of data in (a) are denoted by points connected by lines; the scatter above and below these data denote plus or minus one standard deviation, respectively, of the individual 10-min data sets in that bin.
(c) Individual 10-min averages from FAST (BD), FAST (straight AD), and FAST (curved AD).
(d) Binned averages of data in (c) are denoted by the points connected by lines; the scatter above and below these data denote plus or minus one standard deviation, respectively, of the individual 10-min data sets in that bin.

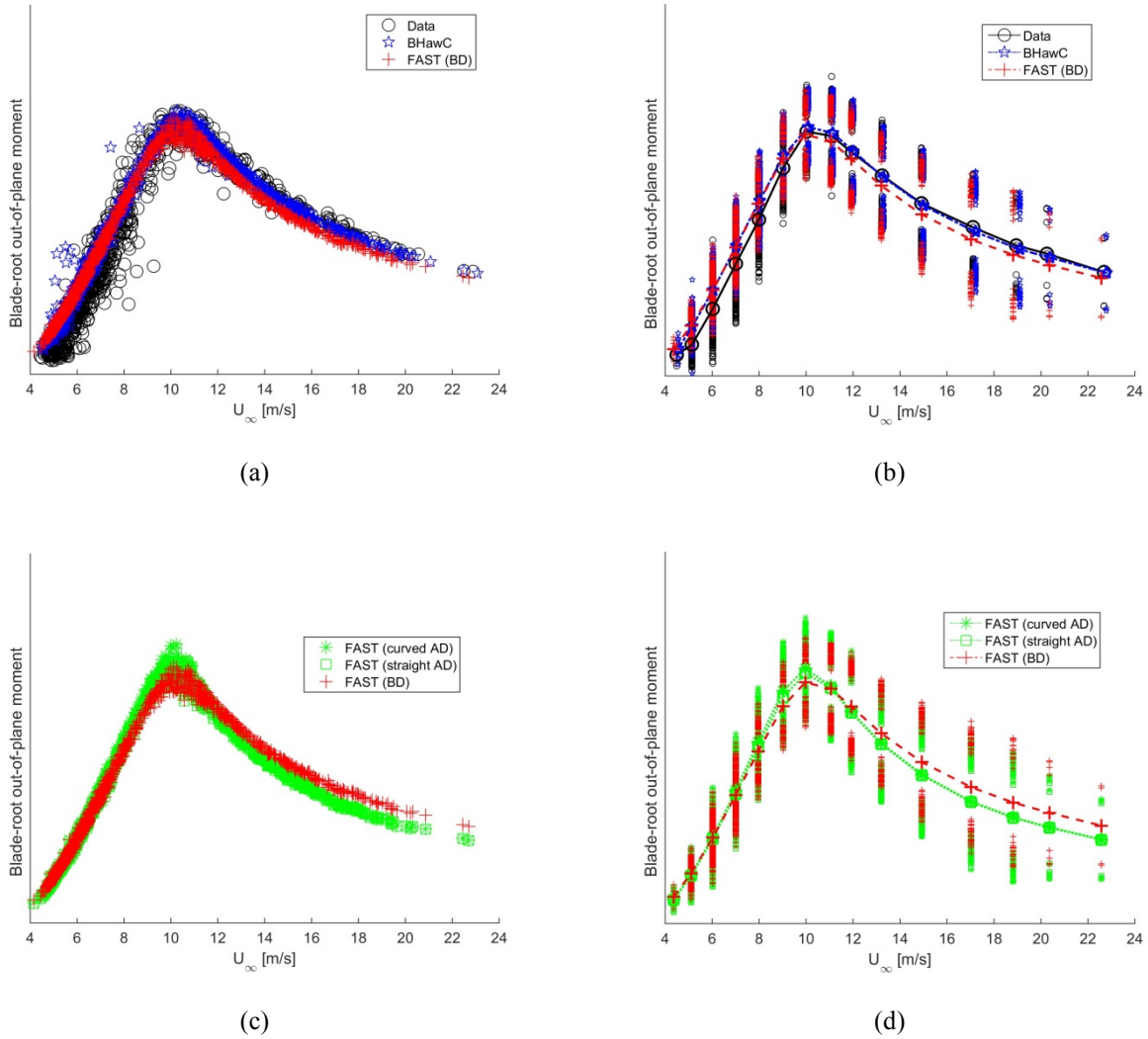

Figure 6: Blade-root out-of-rotor-plane bending moments.
(a) Individual 10-min averages from experimental data, BHawC, and FAST (BD).
(b) Binned averages of data in (a) are denoted by points connected by lines; the scatter above and below these data denote plus or minus one standard deviation, respectively, of the individual 10-min data sets in that bin.
(c) Individual 10-min averages from FAST (BD), FAST (straight AD), and FAST (curved AD).
(d) Binned averages of data in (c) are denoted by the points connected by lines; the scatter above and below these data denote plus or minus one standard deviation, respectively, of the individual 10-min data sets in that bin.

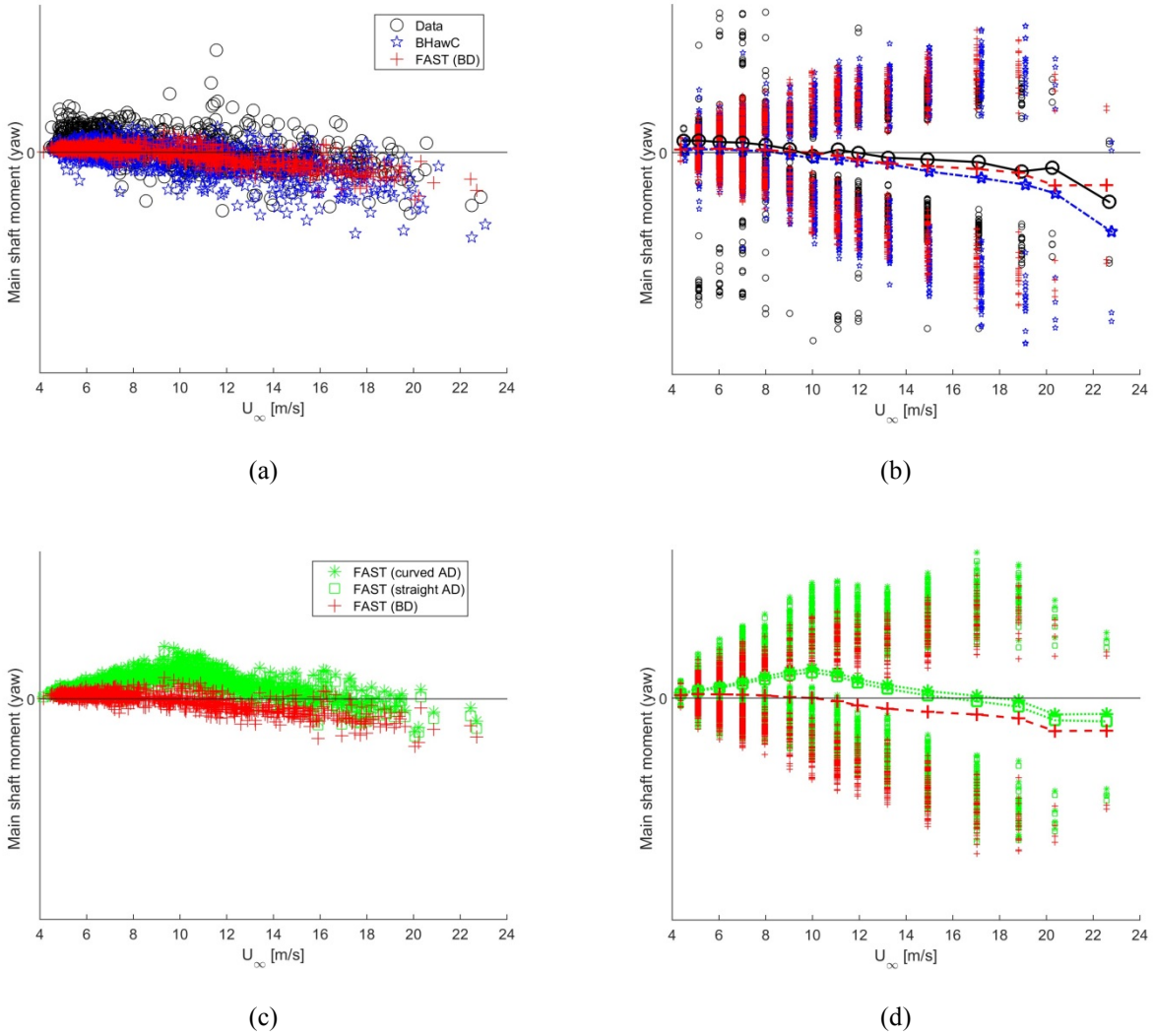

Figure 7: Main shaft bending moment - yaw (non-rotating coordinate system).
(a) Individual 10-min averages from experimental data, BHawC, and FAST (BD).
(b) Binned averages of data in (a) are denoted by points connected by lines; the scatter above and below these data denote plus or minus one standard deviation, respectively, of the individual 10-min data sets in that bin.
(c) Individual 10-min averages from FAST (BD), FAST (straight AD), and FAST (curved AD).
(d) Binned averages of data in (c) are denoted by the points connected by lines; the scatter above and below these data denote plus or minus one standard deviation, respectively, of the individual 10-min data sets in that bin.

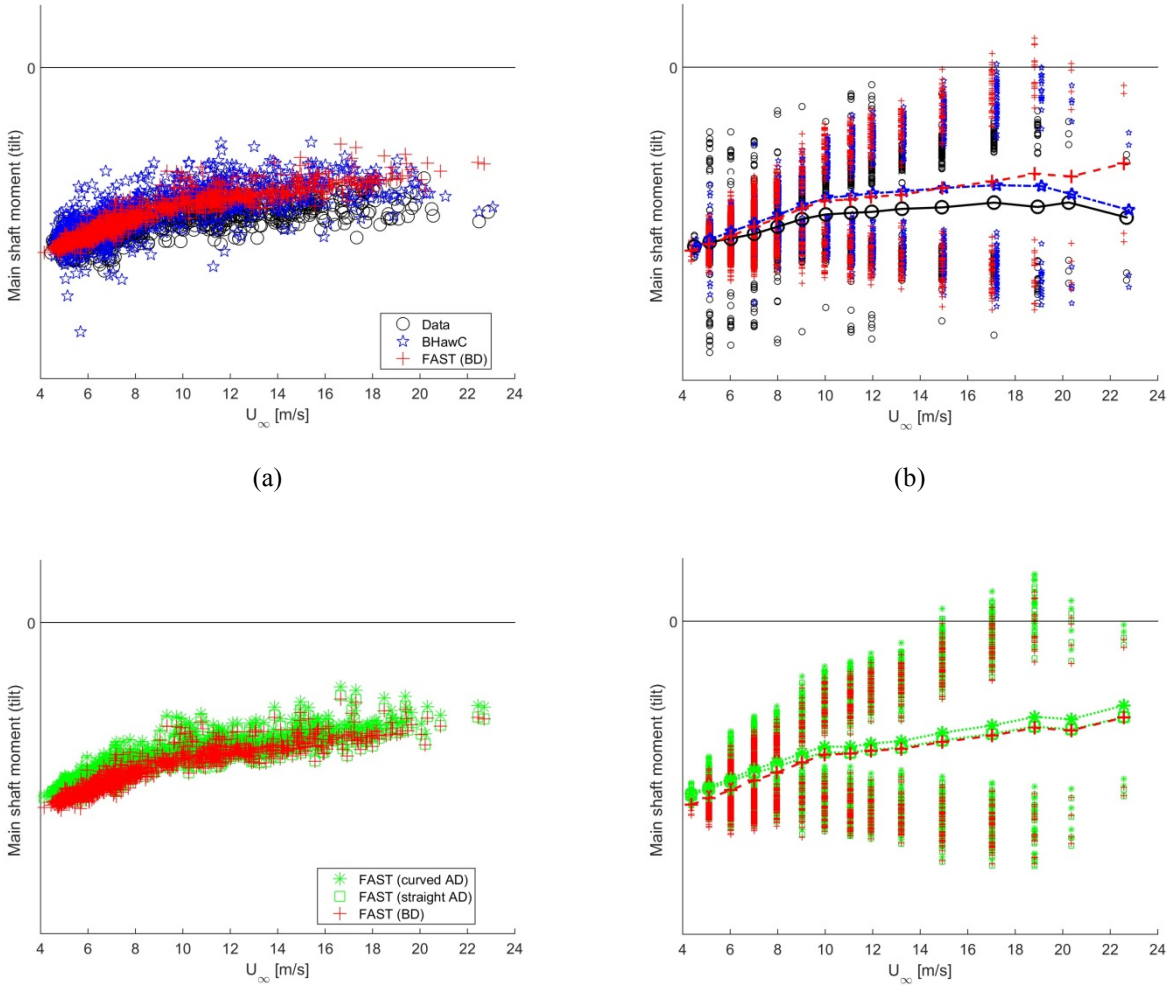

Figure 8: Main shaft bending moment - tilt (non-rotating coordinate system).
(a) Individual 10-min averages from experimental data, BHawC, and FAST (BD).
(b) Binned averages of data in (a) are denoted by points connected by lines; the scatter above and below these data denote plus or minus one standard deviation, respectively, of the individual 10-min data sets in that bin.
(c) Individual 10-min averages from FAST (BD), FAST (straight AD), and FAST (curved AD).
(d) Binned averages of data in (c) are denoted by the points connected by lines; the scatter above and below these data denote plus or minus one standard deviation, respectively, of the individual 10-min data sets in that bin.

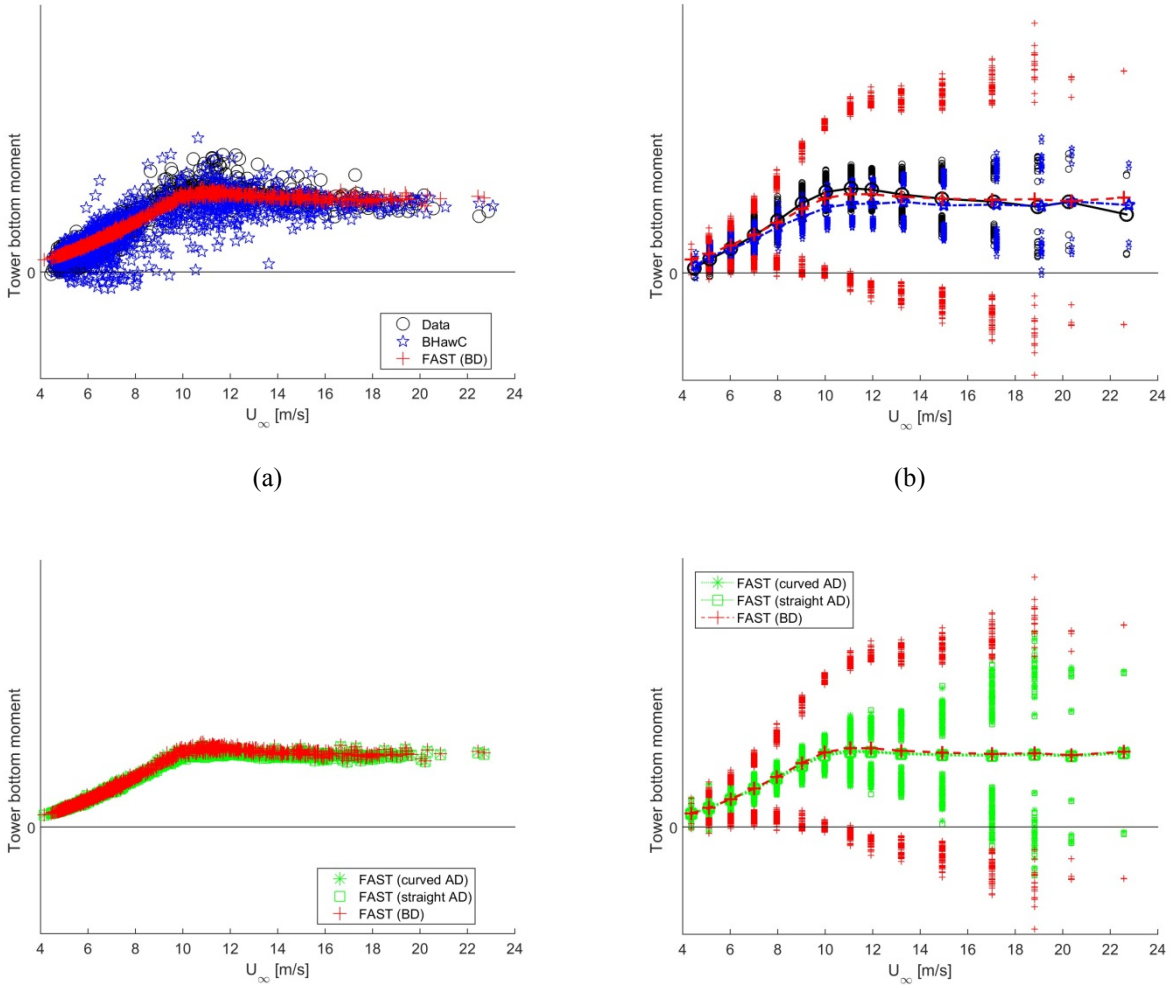

Figure 9: Tower-bottom side-side bending moments.
(a) Individual 10-min averages from experimental data, BHawC, and FAST (BD).
(b) Binned averages of data in (a) are denoted by points connected by lines; the scatter above and below these data denote plus or minus one standard deviation, respectively, of the individual 10-min data sets in that bin.
(c) Individual 10-min averages from FAST (BD), FAST (straight AD), and FAST (curved AD).
(d) Binned averages of data in (c) are denoted by the points connected by lines; the scatter above and below these data denote plus or minus one standard deviation, respectively, of the individual 10-min data sets in that bin.

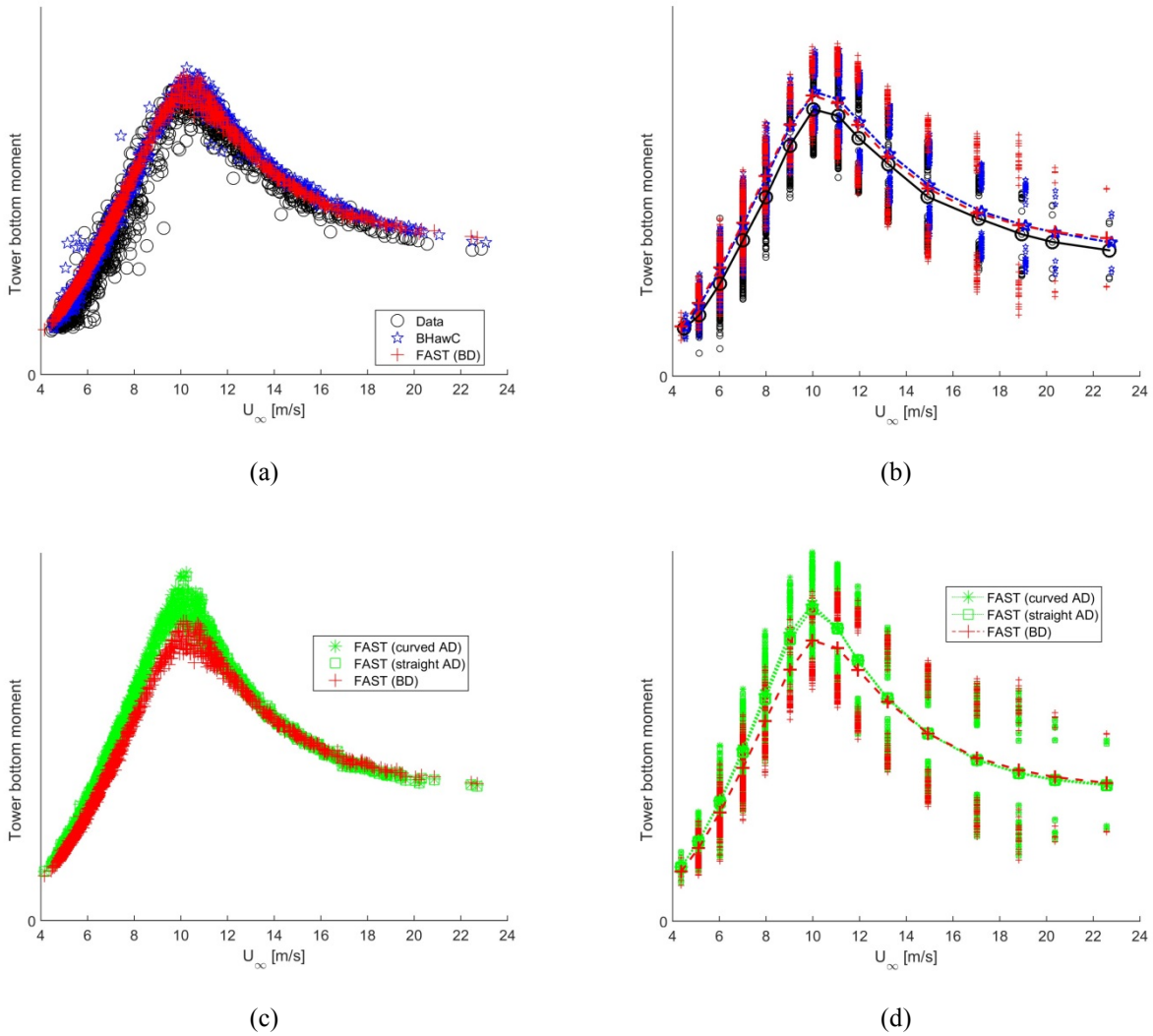

Figure 10: Tower-bottom fore-aft bending moments.
(a) Individual 10-min averages from experimental data, BHawC, and FAST (BD).
(b) Binned averages of data in (a) are denoted by points connected by lines; the scatter above and below these data denote plus or minus one standard deviation, respectively, of the individual 10-min data sets in that bin.
(c) Individual 10-min averages from FAST (BD), FAST (straight AD), and FAST (curved AD).
(d) Binned averages of data in (c) are denoted by the points connected by lines; the scatter above and below these data denote plus or minus one standard deviation, respectively, of the individual 10-min data sets in that bin.

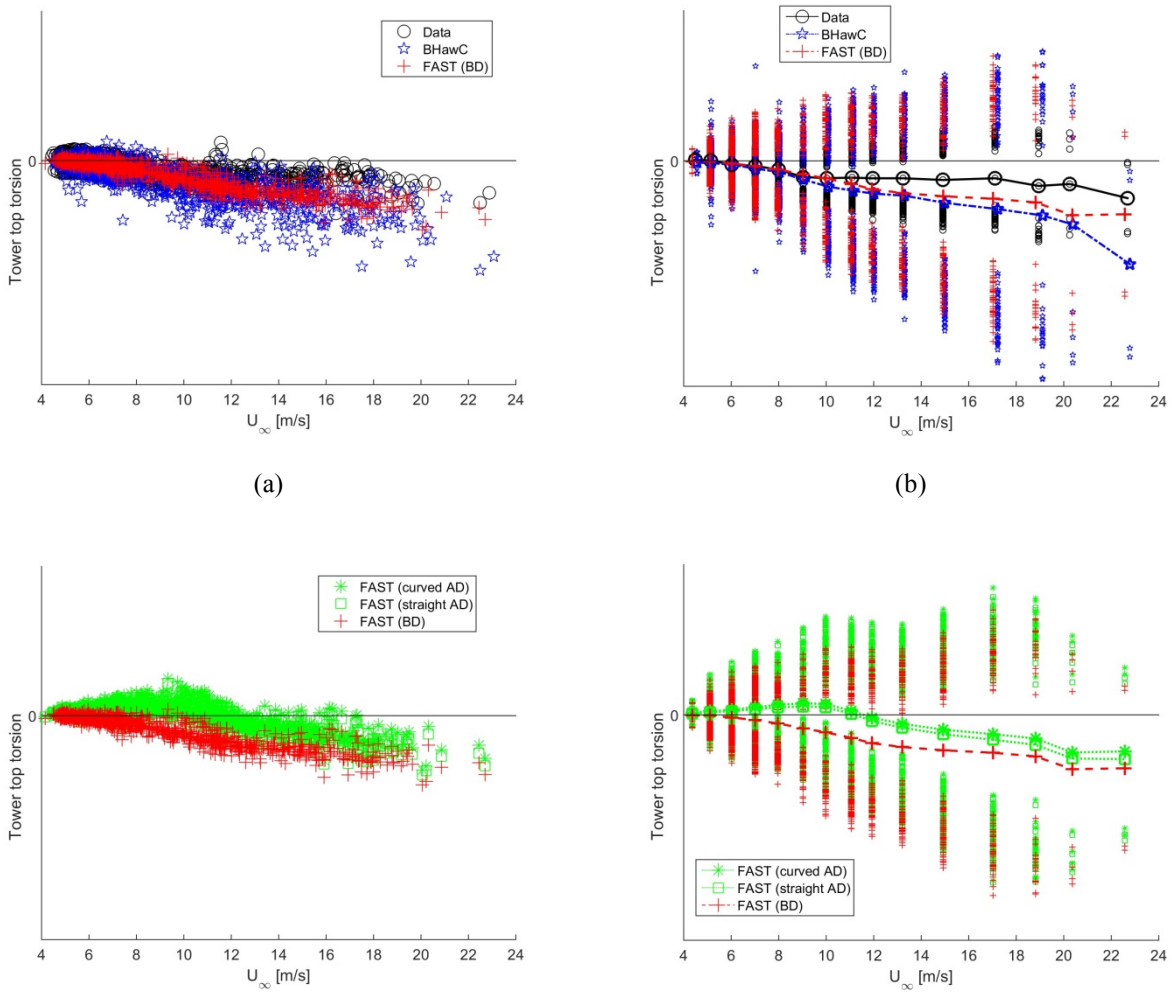

Figure 11: Tower-top torsion moment.
(a) Individual 10-min averages from experimental data, BHawC, and FAST (BD).
(b) Binned averages of data in (a) are denoted by points connected by lines; the scatter above and below these data denote plus or minus one standard deviation, respectively, of the individual 10-min data sets in that bin.
(c) Individual 10-min averages from FAST (BD), FAST (straight AD), and FAST (curved AD).
(d) Binned averages of data in (c) are denoted by the points connected by lines; the scatter above and below these data denote plus or minus one standard deviation, respectively, of the individual 10-min data sets in that bin.

References

1 Jonkman, J., "The New Modularization Framework for the FAST Wind Turbine CAE Tool," 51st AIAA Aerospace Sciences Meeting including the New Horizons Forum and Aerospace Exposition, American Institute of Aeronautics and Astronautics (AIAA), Jan 2013.

2 Sprague, M. A., Jonkman, J. M., and Jonkman, B., "FAST Modular Framework for Wind Turbine Simulation: New Algorithms and Numerical Examples," 33rd Wind Energy Symposium, American Institute of Aeronautics and Astronautics (AIAA), Jan 2015.

3 Wang, Q., Johnson, N., Sprague, M. A., and Jonkman, J. M., "BeamDyn: A High-Fidelity Wind Turbine Blade Solver in the FAST Modular Framework," 33rd Wind Energy Symposium, American Institute of Aeronautics and Astronautics, Jan 2015.

4 Ning, A., Hayman, G., Damiani, R., and Jonkman, J. M., "Development and Validation of a New Blade Element Momentum Skewed-Wake Model within AeroDyn," 33rd Wind Energy Symposium, American Institute of Aeronautics and Astronautics, Jan 2015.

5 IEC 61400-13, "Wind turbine generator systems Part 13: Measurement of mechanical loads," Tech. Rep. IEC 61400-13, Geneva, Switzerland, June 2001.

6 Damiani, R., Haymany, G., Wangz, Q., Jonkman, J., and Gonzalez, A., "Development and Validation of a New Unsteady Airfoil Aerodynamics Model Within AeroDyn," 34th Wind Energy Symposium , American Institute of Aeronautics and Astronautics, San Diego, CA, Jan 2016.

7 Medina, P., Singh, M., Johansen, J., Jove, A., Fingersh, L. J., and Schreck, S., "Inflow Characterization and Aerodynamic Measurements on a SWT-2.3-101 Wind turbine," 50th AIAA Aerospace Sciences Meeting including the New Horizons Forum and Aerospace Exposition, American Institute of Aeronautics and Astronautics (AIAA), Jan 2012.

8 Wang, Q., Sprague, M., Jonkman, J., and Jonkman, B., "Partitioned Nonlinear Structural Analysis of Wind Turbines Using BeamDyn," 34th Wind Energy Symposium, American Institute of Aeronautics and Astronautics, San Diego, CA, Jan 2016.

9 Snel, H., Houwink, R., Bosschers, J., Piers, W., van Bussel, G., and Bruining, A., "Sectional prediction of 3-D effects for stalled flow on rotating blades and comparison with measurements," Proc. of the European Community Wind Energy Conference, March 1993, pp. 395–399.

10 Hills, R. G., Maniaci, D. C., and Naughton, J. W., "V & V Framework," Tech. Rep. SAND2015-7455, Sandia National Laboratories, 2015.